

## DESCRIPTION

<b>Species Reactivity</b>	Mouse
<b>Specificity</b>	Detects mouse LYVE-1 in direct ELISAs and Western blots.
<b>Source</b>	Polyclonal Goat IgG
<b>Purification</b>	Antigen Affinity-purified
<b>Immunogen</b>	Mouse myeloma cell line NS0-derived recombinant mouse LYVE-1 Ala24-Thr234 Accession # Q8BHC0
<b>Formulation</b>	Lyophilized from a 0.2 µm filtered solution in PBS with Trehalose. See Certificate of Analysis for details. *Small pack size (-SP) is supplied either lyophilized or as a 0.2 µm filtered solution in PBS.

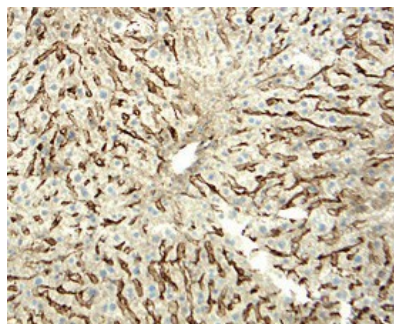
## APPLICATIONS

**Please Note:** Optimal dilutions should be determined by each laboratory for each application. [General Protocols](#) are available in the Technical Information section on our website.

	<b>Recommended Concentration</b>	<b>Sample</b>
<b>Dual RNAscope ISH-IHC Compatible</b>	5-15 µg/mL	Immersion fixed paraffin-embedded sections of mouse liver
<b>Western Blot</b>	0.25 µg/mL	See Below
<b>Immunohistochemistry</b>	5-15 µg/mL	See Below

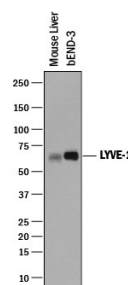
## DATA

### Immunohistochemistry



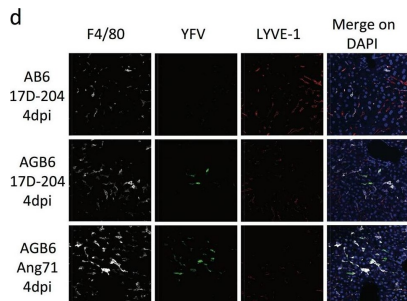
**LYVE-1 in Mouse Liver.** LYVE-1 was detected in perfusion fixed frozen sections of mouse liver using 15 µg/mL Goat Anti-Mouse LYVE-1 Antigen Affinity-purified Polyclonal Antibody (Catalog # AF2125) overnight at 4 °C. Tissue was stained with the Anti-Goat HRP-DAB Cell & Tissue Staining Kit (brown; Catalog # CTS008) and counterstained with hematoxylin (blue). Specific labeling was localized to the cytoplasm of endothelial cells in sinusoids. View our protocol for [Chromogenic IHC Staining of Frozen Tissue Sections](#).

### Western Blot



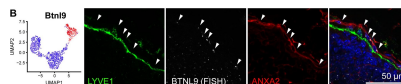
**Detection of Mouse LYVE-1 by Western Blot.** Western blot shows lysates of mouse liver tissue and bEnd.3 mouse brain endothelial cell line. PVDF membrane was probed with 0.25 µg/mL of Goat Anti-Mouse LYVE-1 Antigen Affinity-purified Polyclonal Antibody (Catalog # AF2125) followed by HRP-conjugated Anti-Goat IgG Secondary Antibody (Catalog # HAF019). A specific band was detected for LYVE-1 at approximately 60-65 kDa (as indicated). This experiment was conducted under reducing conditions and using [Immunoblot Buffer Group 1](#).

**Immunocytochemistry/ Immunofluorescence**



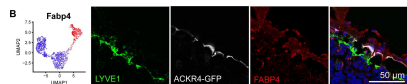
**Detection of Mouse LYVE-1 by Immunocytochemistry/Immunofluorescence** 17D-204 causes viscerotropic abnormalities in the absence of IFN- $\gamma$ . H&E sections (a–c) antibody-stained frozen sections (b, d) of spleen (a, b) and liver (c, d) were presented. a Spleen sections from 17D-204-infected animals were indistinguishable at 4 dpi, whereas Angola71-infected animals display loss of white pulp and red pulp architecture and increase in infiltrating macrophages and neutrophils (inset) at 4 dpi. At 11 dpi, 17D-204 infected AGB6 has increased immune infiltration and extramedullary hematopoiesis (inset) but not AB6 mice. b YFV antigen can be detected in the spleen at 4 dpi in both AB6 and AGB6 mice in the red pulp and outer marginal zone area. c 17D-204-infected AB6 mice do not display major histological changes but infected AGB6 mice and Angola71-infected animals had microsteatosis (inset) at 4 dpi. In AGB6 mice, microsteatosis only occurs transiently at 4 dpi and resolved by 11 dpi. Antibody-stained frozen liver sections (d) revealed that YFV antigen could only be detected in infected AGB6 mice at 4 dpi but not AB6 mice, parallel to titer data in Fig. 1g. Original magnification = 40 $\times$ , n = 4 Image collected and cropped by CiteAb from the following publication (<https://www.nature.com/articles/s41541-017-0039-z>), licensed under a CC-BY license. Not internally tested by R&D Systems.

**Immunocytochemistry/ Immunofluorescence**



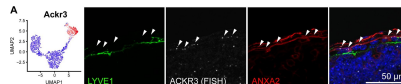
**Detection of Mouse LYVE-1 by Immunocytochemistry/Immunofluorescence** Molecular characterization of LECs in the SCS ceiling with RNA FISH. (A–B) Expression of new cLEC/cluster 2 marker genes Ackr3 (A) and Btl9 (B) by RNA sequencing (left panels) and RNA FISH (right panels). As GFP fluorescence is lost during tissue processing for RNA FISH, immunofluorescence staining for ANXA2 (red) and LYVE1 (green) served as markers for cLECs and fLECs, respectively. Arrows point to cLECs expressing Ackr3 and Btl9 transcripts (white). ACKR3, atypical chemokine receptor 3; ANXA2, annexin A2; Btl9, butyrophilin like 9; cLEC, ceiling LEC; FISH, fluorescence in situ hybridization; fLEC, floor-lining LEC; LEC, lymphatic endothelial cell; LYVE1, lymphatic vessel endothelial hyaluronan receptor 1; SCS, subcapsular sinus; UMAP, Uniform Manifold Approximation and Projection. Image collected and cropped by CiteAb from the following publication (<https://pubmed.ncbi.nlm.nih.gov/32251437>), licensed under a CC-BY license. Not internally tested by R&D Systems.

**Immunocytochemistry/ Immunofluorescence**



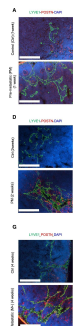
**Detection of Mouse LYVE-1 by Immunocytochemistry/Immunofluorescence** Molecular characterization of LECs in the SCS ceiling with immunofluorescence staining. (A–C) Expression of new cLEC/cluster 2 marker genes ANXA2 (A), FABP4 (B), and CD36 (C) by RNA sequencing (left panels) and immunofluorescence staining (right panels) in Ackr4-GFP reporter mice. GFP (white) and immunofluorescence costaining for LYVE1 (green) served as markers for cLECs and fLECs, respectively. ACKR4, atypical chemokine receptor 4; ANXA2, annexin A2; CD, cluster of differentiation; cLEC, ceiling LEC; FABP4, fatty acid binding protein 4; fLEC, floor-lining LEC; GFP, green fluorescent protein; LEC, lymphatic endothelial cell; LYVE1, lymphatic vessel endothelial hyaluronan receptor 1; SCS, subcapsular sinus; UMAP, Uniform Manifold Approximation and Projection. Image collected and cropped by CiteAb from the following publication (<https://pubmed.ncbi.nlm.nih.gov/32251437>), licensed under a CC-BY license. Not internally tested by R&D Systems.

**Immunocytochemistry/ Immunofluorescence**



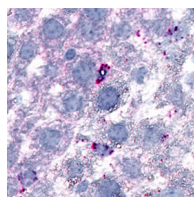
**Detection of Mouse LYVE-1 by Immunocytochemistry/Immunofluorescence** Molecular characterization of LECs in the SCS ceiling with RNA FISH. (A–B) Expression of new cLEC/cluster 2 marker genes Ackr3 (A) and Btl9 (B) by RNA sequencing (left panels) and RNA FISH (right panels). As GFP fluorescence is lost during tissue processing for RNA FISH, immunofluorescence staining for ANXA2 (red) and LYVE1 (green) served as markers for cLECs and fLECs, respectively. Arrows point to cLECs expressing Ackr3 and Btl9 transcripts (white). ACKR3, atypical chemokine receptor 3; ANXA2, annexin A2; Btl9, butyrophilin like 9; cLEC, ceiling LEC; FISH, fluorescence in situ hybridization; fLEC, floor-lining LEC; LEC, lymphatic endothelial cell; LYVE1, lymphatic vessel endothelial hyaluronan receptor 1; SCS, subcapsular sinus; UMAP, Uniform Manifold Approximation and Projection. Image collected and cropped by CiteAb from the following publication (<https://pubmed.ncbi.nlm.nih.gov/32251437>), licensed under a CC-BY license. Not internally tested by R&D Systems.

### Immunocytochemistry/ Immunofluorescence

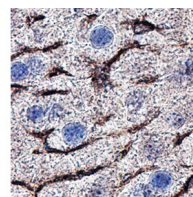


**Detection of Mouse LYVE-1 by Immunocytochemistry/Immunofluorescence** POSTN is upregulated in (pre)-metastatic LN. Morphometric analysis of POSTN and LYVE1+ lymphatic vessels in experimental (pre)-metastatic LN (in the ear sponge assay using B16F10 cells). CTRLs correspond to mice implanted with a sponge without tumor cells. a–d–g Immunostaining of POSTN (red) and LYVE1 (green) in pre-metastatic (PM) (at 1 week in A, at 2 weeks in d) and in metastatic (M+) LNs (G). Bars = 250  $\mu$ m. b–e–h Scatter graphs use scatter plots to represent POSTN and LYVE1 densities (in percentage) assessed by a computer assisted method ( $n \geq 9$ ). Results are expressed as mean  $\pm$  SD, and statistical analyses were performed using a Wilcoxon–Mann–Whitney test (\* $p < 0.05$ ; \*\* $p < 0.01$ ; \*\*\* $p < 0.001$ ; \*\*\*\* $p < 0.0001$ ). c–f–i Spatial distribution analysis from tissue edge to tissue center. The blue rectangle indicates the area between 0–0.30 mm from the LN border where the cumulate normalized areas of LYVE1 and POSTN were measured and represented in the top right. Maximum distance of migration from the tissue border (Lmax) is indicated. Results are expressed as mean  $\pm$  SD (Wilcoxon–Mann–Whitney test: \* $p < 0.05$ ; \*\* $p < 0.01$ ). d–i All the results represent the set of two independent experiments Image collected and cropped by CiteAb from the following publication (<https://pubmed.ncbi.nlm.nih.gov/35567669/>), licensed under a CC-BY license. Not internally tested by R&D Systems.

### In-situ Hybridization



In Situ Hybridization (ISH)



Immunohistochemistry (IHC)

**Detection of LYVE-1 in Mouse Liver.** Formalin-fixed paraffin-embedded tissue sections of mouse liver were probed for LYVE1 mRNA (ACD RNAScope Probe, catalog # 428451; Fast Red chromogen, ACD catalog # 322360). Adjacent tissue section was processed for immunohistochemistry using goat anti-mouse LYVE1 polyclonal antibody (R&D Systems catalog # Catalog # AF2125) at 5 $\mu$ g/mL with overnight incubation at 4 degrees Celsius followed by incubation with anti-goat IgG VisUCyte HRP Polymer Antibody (Catalog # Catalog # VC004) and DAB chromogen (yellow-brown). Tissue was counterstained with hematoxylin (blue). Specific staining was localized to endothelial cells of sinusoids.

### PREPARATION AND STORAGE

<b>Reconstitution</b>	Reconstitute at 0.2 mg/mL in sterile PBS. For liquid material, refer to CoA for concentration.
<b>Shipping</b>	Lyophilized product is shipped at ambient temperature. Liquid small pack size (-SP) is shipped with polar packs. Upon receipt, store immediately at the temperature recommended below.
<b>Stability &amp; Storage</b>	<p><b>Use a manual defrost freezer and avoid repeated freeze-thaw cycles.</b></p> <ul style="list-style-type: none"> <li>12 months from date of receipt, -20 to -70 °C as supplied.</li> <li>1 month, 2 to 8 °C under sterile conditions after reconstitution.</li> <li>6 months, -20 to -70 °C under sterile conditions after reconstitution.</li> </ul>

### BACKGROUND

Lymphatic vessel endothelial hyaluronan (HA) receptor-1 (LYVE-1) is a recently identified receptor of HA, a linear high molecular weight polymer composed of alternating units of D-glucuronic acid and N-acetyl-D-glucosamine. HA is found in the extracellular matrix of most animal tissues and in body fluids. It modulates cell behavior and functions during tissue remodeling, development, homeostasis, and disease. The turnover of HA (several grams/day in humans) occurs primarily in the lymphatics and liver, the two major clearance systems that catabolize approximately 85% and 15% of HA, respectively. LYVE-1 shares 41% homology with the other known HA receptor, CD44. The homology between the two proteins increases to 61% within the HA binding domain. The HA binding domain, known as the link module, is a common structural motif found in other HA binding proteins such as link protein, aggrecan and versican. Human and mouse LYVE-1 share 69% amino acid sequence identity.

LYVE-1 is primarily expressed on both the luminal and abluminal surfaces of lymphatic vessels. In addition, LYVE-1 is also present in normal hepatic blood sinusoidal endothelial cells. LYVE-1 mediates the endocytosis of HA and may transport HA from tissue to lymph by transcytosis, delivering HA to lymphatic capillaries for removal and degradation in the regional lymph nodes. Because of its restricted expression patterns, LYVE-1, along with other lymphatic proteins such as VEGF R3, podoplanin and the homeobox protein prospero-related (Prox-1), constitute a set of markers useful for distinguishing between lymphatic and blood microvasculature.